euspen's 21st International Conference & Exhibition, Copenhagen, DK, June 2021
www.euspen.eu

Focused ion beam writing of submicron structures into coated mold inserts

Holger Ruehl[1], Michael Haub[1], Serhat Sahakalkan[2], Thomas Guenther[1,2], André Zimmermann[1,2]

[1]*University of Stuttgart, Institute for Micro Integration (IFM), Allmandring 9b, 70569 Stuttgart, Germany*
[2]*Hahn-Schickard e.V., Allmandring 9b, 70569 Stuttgart*

Submitting author: holger.ruehl@ifm.uni-stuttgart.de

Abstract
Molding techniques allow the replication of surface structures to enable improved or novel functions for optics, fluidics and further applications. In general, the molding process can be facilitated by means of antiadhesive-coated molds due to a reduction of demolding forces, wear or prevention of heat dissipation. Consequently, employing coated molds, an improved demolding of features with submicron dimensions and high aspect ratio can be expected. In order to achieve adequate results regarding the replication of nanostructures, accurate mastering techniques to structure the coating are required. One possible technique is focused ion beam (FIB) writing, which was investigated in this study regarding its suitability to mill structured surfaces of submicron dimensions into coated mold inserts. Mold inserts were coated with a thin-film diamond-like carbon (DLC) and chromium nitride (CrN) as well as electroless plated nickel-phosphorus (NiP). The coatings were examined by means of SEM imaging and roughness measurements regarding their applicability for the creation of nanostructures. Subsequently, a test pattern was written into the coatings using a FIB-SEM dual beam system. The test pattern consisted of the USAF test chart target groups 9, 10 and a Siemens star. The lateral dimensions were ≤ 980 nm. During ion beam milling, the beam parameters current and the number of scan repetitions were varied to investigate their influence on the structuring result. Subsequently, SEM measurements were conducted to characterize the milled nanostructures. Different lateral resolutions and depths of the pattern and effects like redeposition or the proximity effect were observed for the nanostructures depending on the coating and processing conditions. Lateral feature sizes down to 60 nm could be realized. In conclusion, the gained results approved FIB writing as a suitable technique to manufacture highly precise nanostructures into surface coatings for molding.

Keywords : Structured surface, surface patterning, antiadhesive, coating, thin-film, diamond-like carbon, FIB, focused ion beam writing, nanostructuring, molding (moulding), micro- and nanoreplication, SEM

1. Introduction

Molding processes enable a cost effective and rapid replication of parts with micro- and nanostructured surfaces. Structured surfaces are used in optics for example as antireflective structures [1] or optical gratings [2]. In fluidics, nano channels are used for the handling of single molecules [3]. In this regard, multiscale structured surfaces must be mentioned as an innovative trend [4]. Metasurfaces on plastic parts present another emerging field, whereas the replicated nanostructures provide improved or novel functions [5,6].

However, the replication of nanostructures by molding is difficult to obtain. During the process, the filling of nanocavities can be incomplete, small features can be easily damaged during demolding or residues remain within the structures, thus damaging any subsequent part in terms of functionality.

Studies showed that by applying thin film coatings on molds, demolding forces [7-9], excessive wear [10,11] or heat dissipation [12] can be reduced. To replicate submicron structures from coated molds, proper mastering techniques for the structuring are needed. For this, it is distinguished between indirect and direct structured molds [13]. For direct coating structuring, there are only a few studies available yet [14,15]. One possible technique could be focused ion beam writing (FIB), which was investigated in this study.

The advantages of FIB are a high flexibility in patterning due to the direct structuring process, a high resolution to create submicron structures as well as a broad range of manufacturable materials [16]. Moreover, by using FIB-SEM dual beam systems, various structures can be created and characterized with the same instrument.

In this study, three different thin film coatings were applied on mold inserts. Subsequently, a test pattern was milled into the coatings under the variation of the FIB parameters to investigate achievable quality and occuring effects.

In the following the experimental design, results and discussion as well as a summary are described one after the other.

2. Experimental

An existing mold insert design for injection compression molding (ICM) with a surface area of 13.3 x 10.3 mm was used [15]. The mold inserts were manufactured by milling. Prior to the coating, the insert surfaces were diamond polished to create optical surface quality with Ra ≤ 10 nm.

The samples were then coated with a tetrahedral hydrogenfree amorphous carbon film (DLC ta-C), chromium nitride (CrN) and electroless nickel-phosphorus (NiP). For the DLC ta-C, the SAM 3000 coating (SAM Coating GmbH, Germany) was arc deposited. BALIQ Cronos (Oerlikon Balzers Coating Germany GmbH, Germany) was applied for CrN in a high power impulse magnetron sputtering (HiPIMS) process. NiP with 12 – 14 % phosphorus content was electroless plated (CZL Tilburg bv, Netherlands) and subsequently smoothed by fly cutting as described in [15]. The roughness of the coated surface was analysed by using a laser probe measuring system (Mitaka MLP-3, Mitaka Kohki Co., Ltd., Japan).

A test pattern consisting of submicron structures, in specific the USAF test chart groups 9, 10 and a Siemens star, was created. Fig. 1 shows the test pattern. The biggest feature size was 980 nm for the width of USAF group 9 element 1. The smallest feature size was 275 nm for the width of USAF group 10 element 6. The width of each star spoke was 980 nm, too.

The test pattern was written into the coated mold inserts in the BITMAP patterning mode. A FIB Helios NanoLab 600 dual beam system with Ga^+ ion beam was used. The acceleration voltage was 30 kV. The ion dose was 1337 pC/µm² for ta-C and CrN as well as 266 pC/µm² for NiP. The dwell time was set to 1 µs. The pixel pitch was 50 %. In a first trial, the aperture (beam current I) and repetition number n were varied. Second, the repetition number n was varied for a fixed beam current of 90 pA (DLC ta-C, CrN) and 46 pA (NiP) in order to investigate effects with creating high aspect ratios. The FIB parameters are given in Table 1 and Table 2. Finally, the milled submicron structures were characterized with the SEM unit of the dual beam system.

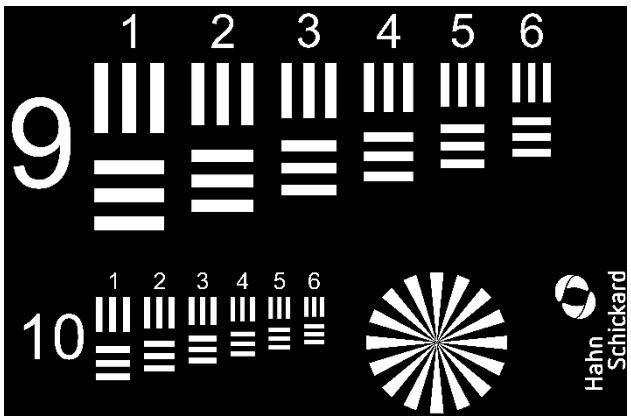

Figure 1. Test pattern consisting of USAF test chart groups 9 and 10, a Siemens star and the laboratory logo for FIB experiments

Table 1 FIB parameters for DLC ta-C and CrN

1	**I [pA]**	260	90	46	26	9
	n	1130	1948	2569	2761	6068
2	**I [pA]**	90				
	n	1948		3884	7769	

Table 2 FIB parameters for NiP

1	**I [pA]**	260	90	46	26	9	1.5
	n	225	389	512	665	1213	2844
2	**I [pA]**	46					
	n	512		1024		2048	

3. Results and Discussion

The measured surface roughness of DLC ta-C was Ra = 10.6 nm and Rq = 13.7 nm and was sufficiently smooth for the FIB experiments. The CrN surface roughness was Ra = 7.5 nm and Rq = 9.8 nm. The smoothest surface was the fly cutted NiP with Ra < 3 nm and Rq < 4 nm. In Fig. 2, the CrN coated mold insert is exemplarily shown.

Figure 2. CrN coated mold insert

3.1. Diamond-like carbon ta-C

Fig. 3 shows the FIB written test pattern into DLC ta-C at an ion beam current I = 260 pA and I = 26 pA. The surfaces inside the nanostructures are fully smooth for all beam currents, which might be due to an isotropic material removal caused by the amorphous ta-C structure. Two effects can be observed when compared the test structures written with 260 pA and 26 pA. First, a lateral rounding of the corners of the single test pattern elements can be seen for higher beam currents. This effect might be caused by the lower resolution of the beam at higher beam currents. Within the 260 pA test structure, a blurring of the smaller elements can be seen so that single elements are not longer recognizable individually, e.g. USAF group 10 Element 5. Second, a clear rounding of the inner and outer edges can be seen at higher beam currents. This effect might be caused by the Gaussian beam profile [2]. For smaller beam currents, these two effects become less significant and the dimensional and shape accuracy improves. For I = 26 pA, all test pattern elements are individually identifiable and of sharp inner and outer edges.

The best shape accuracy is achieved at I = 9 pA. For this beam current, the smallest feature width is 63 nm, measured in a Siemens star spoke. However, the milling time for the USAF group 10 and the Siemens star written at I = 9 pA is almost equal to the milling time for the entire test pattern written at I = 26 pA. The choice of aperture should therefore carefully be determined by the required shape accuracy and processing time.

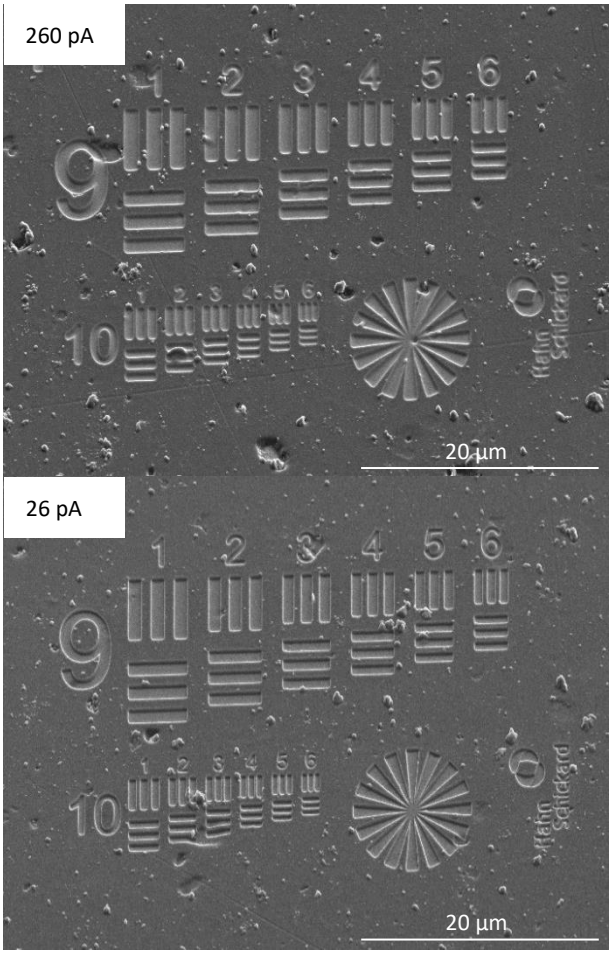

Figure 3. Focused ion beam written test patterns into tetrahedral hydrogenfree amorphous diamond-like carbon at beam current I = 260 pA and I = 26 pA

Also for the varied number of scans, two effects can be observed. Fig. 4 shows the Siemens stars milled with n = 1948 and n = 7769. For n = 1948, the structure depth is around 300 nm with vertical sidewalls. In contrast, for n = 7769 the depth is around 800 nm and the sidewalls are inclined. From this, redeposition effects can be seen for higher aspect ratios. Furthermore, a dropping of the Siemens star spokes towards the center of the star with a full exposure of the star center is seen for high aspect ratios which might be caused by proximity effects [2,16].

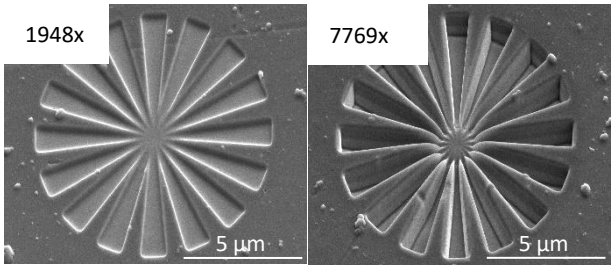

Figure 4. Focused ion beam written Siemens stars into tetrahedral hydrogenfree amorphous diamond-like carbon at beam current at I = 90 pA and n = 1948 and n = 7769

3.2. Chromium Nitride

Fig. 5 shows the FIB written test pattern into chromium nitride at an ion beam current I = 260 pA and I = 26 pA. Since the deposited CrN is of crystalline structure, the material removal is anisotropic and thus, channeling occurs. While the structure width is dimensionally stable at I = 260 pA, the channeling effects the dimensional accuracy for lower beam currents resulting in narrower structure widths. Channeling also effects the surface roughness of the structure. On the one side the surface roughness of the sidewall is smoothed for smaller beam currents, while roughening occurs at the bottom of the structures resulting in different structure depths. Redeposition is lowered which might be due to the reduced sputtering yield per scan repetition.

Fig. 6 shows the Siemens stars milled with repetition number n = 1948 and n = 7769. It can be seen that redeposition and proximity effects occur at higher aspect-ratios.

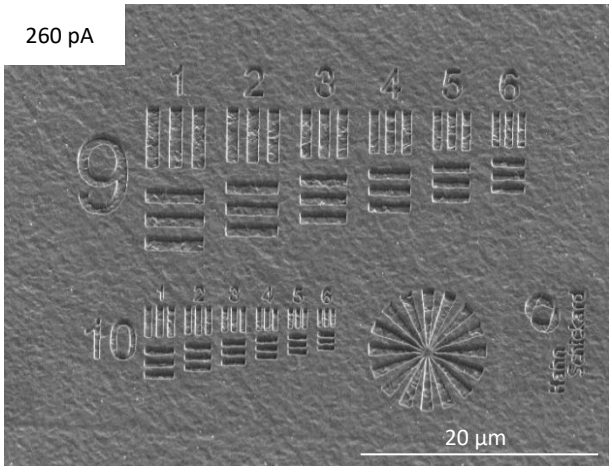

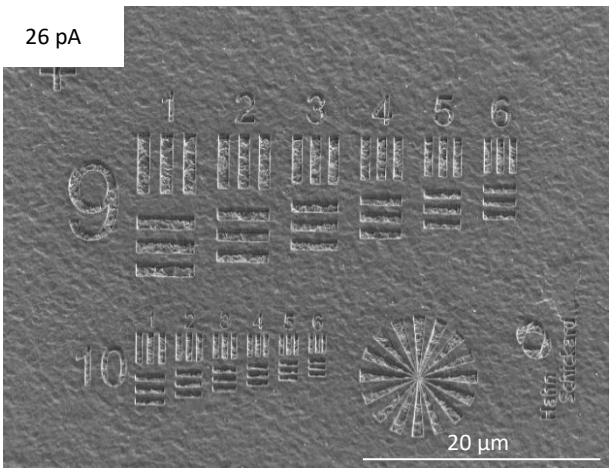

Figure 5. Focused ion beam written test patterns into chromium nitride at beam current I = 260 pA and I = 26 pA

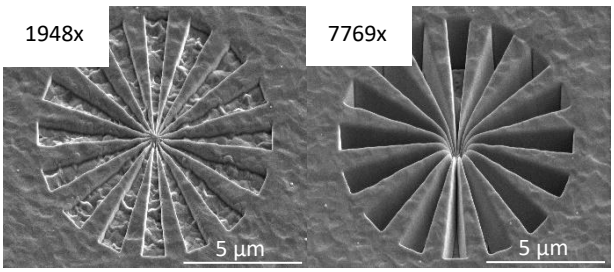

Figure 6. Focused ion beam written Siemens stars into tetrahedral hydrogenfree amorphous diamond-like carbon at beam current at I = 90 pA and n = 1948 and n = 7769

3.3. Nickel-Phosphorus

Fig. 7 shows the FIB written test pattern into fly-cutted NiP at an ion beam current I = 260 pA and I = 1.5 pA. NiP can be machined via FIB at a lower ion dose compared to DLC ta-C or CrN. However, due to a processing time longer than 2 h, only the USAF test chart group 10 and the Siemens star were milled at I = 1.5 pA.

The roughness inside the nanostructures is morphologically equal to the non-structured areas. The smoothness might be caused by an isotropic sputtering due to the amorphous structure. The shape accuracy improves for smaller beam currents due to the higher resolution of the ion beam. The inner and outer edges of the nanostructures are rounded, which might be affected by the beam profile, but not by redeposition since this effect did not intensify at smaller beam currents.

From I = 46 A, already sputtered material is redeposited at the test pattern sidewalls with the adjusted beam settings. This effect intensifies for small beam currents with the scanning direction from left to right and vice versa, leading to a filling of the smallest structures. For I = 1.5 pA, the USAF test chart elements and the spoke ends of the Siemens star are filled with redeposited material as shown in Fig. 7. The redeposition could be diminished by minimizing the dwell time to fasten the writing speed leading to a lowered sputtering yield per scan.

Fig. 8 shows the Siemens stars milled with n = 512 and n = 2048. It can be seen, that proximity effects cause a too high exposure of the star center limiting the smallest lateral feature size at high aspect ratios as it is seen for DLC ta-C and CrN. However, redeposition is only marginally recognizable.

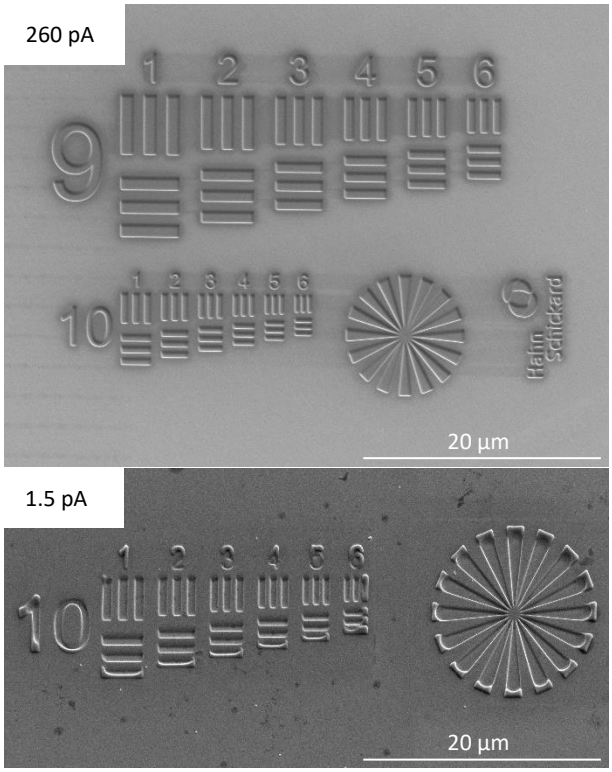

Figure 7. Focused ion beam written test patterns into nickel-phosphorus at beam current I = 260 pA and I = 1.5 pA

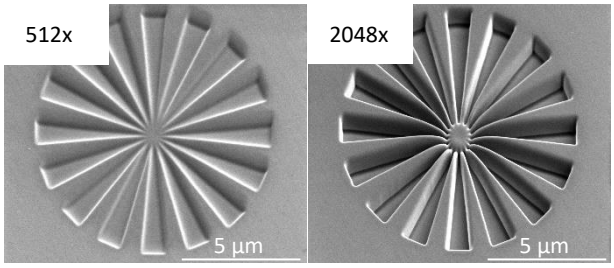

Figure 8. Focused ion beam written Siemens stars into electroless plated nickel-phosporus at beam current at I = 46 pA and n = 512 and n = 2048

4. Summary

In this study, mold inserts for ICM were coated with DLC ta-C, CrN und NiP. Subsequently, submicron structures were successfully focused ion beam written into the coatings.

Depending on the coating material and FIB processing conditions, different effects occurred. For all coatings, the lateral resolution of the test pattern improved with smaller beam currents. The smallest, measured feature size was 63 nm. With rising aspect ratio, redeposition induced typical V-shaped sidewalls. For structure sizes smaller than 200 nm in combination with highest aspect ratios, the proximity effect caused additional lateral material removal as it was seen for the Siemens stars milled in DLC-taC and NiP. Channeling determined the shape of the written submicron structures in the crystalline CrN, whereas isotropic sputtering was seen for amorphous coatings (ta-C, NiP).

As a next step, the nanostructured surfaces onto the coatings are to be replicated via ICM in order to study the influence of the coating on the molding process under variation of the process conditions (e.g. isothermal/variothermal molding, different molding parameters, vacuum yes/no).

Further research deals with the investigation of the influence of other FIB parameters, that have not yet been investigated within the scope of this study, e.g. dwell time or irradiation angle. Furthermore the grayscale FIB milling into the coatings is under investigation in order to create 3D structures.

References

[1] Christianssen A B, Højlund-Nielsen E, Clausen Jeppe, Caringal G P, Asger Mortensen N and Kristensen A 2013 Imprinted and injection-molded nano-structured optical surfaces *Nanostructured Thin Films VI* **8818** 03
[2] Keskinbora K 2019 *Prototyping Micro- and Nano-Optics with Focused Ion Beam Lithography* **SL48** 46
[3] Calaon M, Tosello G, Garnaes J and Hansen H N 2017 Injection and injection-compression moulding replication capability for the production of polymer lab-on-a-chip with nano structures *J. Micromech. Microeng.* **27** 2015001
[4] Brinksmeier E, Karpuschewski B, Yan J, Schönemann L 2020 Manufacturing of multiscale structured surfaces *CIRP Annals - Manufacturing Technology* **69** 717
[5] Højlund-Nielsen E, Clausen J, Mäkela T, Højlundd Thamdrup L, Zalkovskij M, Nielsen T, Li Pira N, Ahopelto J, Asger Mortensen N and Kristensen A 2016 Plasmonic Colors: Toward Mass Production of Metasurfaces *Adv. Mater. Technol.* **1** 1600054
[6] Zhu X, Yan W, Levy U, Asger Mortensen N and Kristensen A 2017 Resonant laser printing of structural colors on high-index dielectric metasurfaces *Sci. Adv.* **3(5)**
[7] Burkard E, Walther T, Schinköthe W 1999 Influence of mold wall coatings while demoulding in the injection molding process Stuttgarter Kunststoff-Kolloquium **16**
[8] Tillmann W, Stangier D, Dias L, Gelinski N, Stanko M, Stommel M, Krebs E and Biermann D 2019 Reduction of Ejection Forces in Injection Molding by Applying Mechanically Post-Treated CrN and CrAlN PVD Films *J. Manuf. Mater. Process.* **3(4)** 88
[9] Charmeau J, Chailly M, Gilbert V and Béreaux Y 2008 Influence of Mold Surface Coatings in Injection Molding. Application to the Ejection Stage Int. J. Mater. Form **1** 699
[10] Griffiths C A, Dimov S S, Rees A, Dellea O, Gavillet J, Lacan F and Hirshy H 2013 A novel texturing of micro injection moulding tools by applying an amorphous hydrogenated carbon coating *Surface and Coatings Technology* **235** 1
[11] D'Avico L, Beltrami R, Lecis and Trasatti S P 2018 Corrosion Behavior and Surface Properties of PVD Coatings for Mold Technology Applications Coatings **9(1)** 7
[12] Stormonth-Darling J M, Pedersen R H, How C and Gadegaard N 2014 Injection moulding of ultra high aspect ratio nanostructures using coated polymer tooling *J. Micromech Microeng.* **24(7)** 75019
[13] Dumitru G, Romano V, Weber H P, Pimenov S, Kononenko T, Hermann J, Bruneau S, Gerbig Y and Shupegin M 2003 Laser treatment of tribological DLC films *Diamond and Related Materials* **12** 1034
[14] Vera J, Brulez A, Contraires E, Larochette M, Trannoy-Orban N, Pignon M, Mauclair C, Valette S and Benayoun S 2018 Factors influencing microinjection molding replication quality *J. Micromech. Microeng.* **28** 05004
[15] Roeder M, Drexler M, Rothermel T, Meissner T, Guenther T and Zimmermann A 2018 Injection Compression Molded Microlens Arrays for Hyperspectral Imaging *Micromachines* **9** 355
[16] Watt F, Bettiol A A, Van Kan J A, Teo E J and Breese M B H 2005 Ion Beam Lithography and Nanofabrication: A Review *Int. J. Nanosci.* **4(3)** 269
[17] Seniutinas G, Gervinskas G, Anguita J, Hakobyan D, Brasselet E and Juodkazis S 2016 Nano-proximity direct ion beam writing *Nanofabrication* **1** 345